Lidar return structure at multiple scattering in the small-angle approximation

V.V. Veretennikov

Institute of Atmospheric Optics,
Siberian Branch of the Russian Academy of Sciences, Tomsk

Received February 8, 1999

The equation for lidar return power is considered, in a small-angle approximation, with the allowance for the dependence of multiple scattering contribution on the disperse medium composition. The ratio between the multiply and singly scattered components of radiation is numerically studied for different optical thickness of a layer depending on the receiver field of view. The applicability of the diffraction approximation for the small-angle part of scattering phase function is estimated when describing lidar returns with the allowance for multiple scattering.

During the last decades lidars have been playing an increasingly important role in atmospheric optics studies. At present a comprehensive theory is developed and efficient methods are constructed for lidar return interpretation in the single scattering approximation.[1–3] When sounding optically dense media, the part of multiply scattered light in lidar return increases greatly and gradually becomes to be dominant. The multiple scattering plays a decisive role in light propagation through large-size media, in which the phase function is strongly forward peaked.

The available algorithms for interpreting the data of laser sensing of dense media are based, as a rule, on separating the lidar return component due to single scattering and on solving this equation for this component using known methods.[4–5] In this case the contribution coming from multiple scattering is considered as noise, which is taken into account by the iteration procedure.

The level of noise due to multiple scattering in lidar returns depends on the optical characteristics of the medium and the experiment geometry. For its rigorous consideration the solution of the radiative transfer equation (RTE) is required that is connected with bulky calculations and makes the operative interpretation of the experimental data difficult.

One of the promising approach, which allows one to overcome these difficulties, is the use of analytical solutions of the radiative transfer equation obtained in the small-angle approximation.[6,7] In Refs. 8–10 the authors proposed and developed some methods for treatment of the multiple scattering in the small-angle approximation to description of lidar returns with the subsequent calculation of the scattering in the large-angle approximation. However, the application of the results obtained in Refs. 8–10, when solving the inverse problems of lidar sensing, is too difficult because the used model descriptions of the scattering phase functions are of extremely simplified form and do not represent real information on the disperse composition of the medium.

This drawback can be overcome using the connection between the scattering phase function of large-size particles in the Fraunhofer diffraction approximation and the geometric parameters of these particles shadow.[11] Such an approach makes it possible to express analytically the dependence of multiple scattering contribution to lidar returns on the parameters of medium microstructure.[12] In its turn, introduction of this dependence into the description of lidar return signals enables one to consider multiple scattering background not as noise but as an extra source of information about the characteristics of the medium sounded, which can be considered when developing the algorithms for lidar data interpretation. Finally, the above approach enables one to predict the behavior of lidar returns given the scattering phase functions corresponding to typical aerosol size-distributions that is necessary in experiments on sounding dense media and in development of the corresponding experimental techniques.

This paper describes the structure of lidar returns depending on the experimental geometry based on the generalization of lidar equation with the allowance made for multiple scattering in the small-angle approximation. The calculated behavior of the multiple scattering background in response to variations of the receiver's field-of-view angle is presented in regard to the disperse composition of scattering media.

1. Formulation of the lidar equation with regard to multiple scattering in the small-angle approximation

This section describes analytical approaches to description of the interconnection between the lidar return power, at the receiver input, and optical characteristics of a disperse medium with the account of contribution from multiple scattering in the small-angle approximation.

Now we shall consider the scattering medium with a forward peaked phase function and the optical characteristics depending only on the single spatial coordinate z. Let us assume that the medium is irradiated with a pulsed radiation from the lidar; the source and the receiver of laser radiation are placed in the plane $z = 0$, their optical axes are parallel to the axis Oz, the distance between the axes equals d, and the

0235-6880/99/05 369-07 $02.00

sensitivity of the receiving system is described by the function $D(\mathbf{r}, \gamma)$ having circular symmetry over the spatial and angular coordinates, where $\mathbf{r}(x, y)$ are the transverse coordinates in the plane $z = 0$ and γ is the angle formed by a given direction with the axis Oz.

We proceed from quite a commonly used model. According to this model, the multiply scattered radiation is taken into account in the vicinity of the direction of propagation of a sounding pulse, and the large scattering angle is considered in the single-scattering approximation. In this case the process of pulse propagation can be subdivided into three stages including the radiation propagation from a source to a scattering volume, where single scattering of the pulse occurs in the backward direction, as well as the scattered radiation propagation from this volume to the receiver. In this case the process of light pulse propagation in both directions is described by the nonstationary radiative transfer equation in the small-angle approximation. The formal description of a lidar return can be obtained with the procedure[8,9] of a successive consideration of large angle scattering. A simple solution is obtained in the case when the variation of the scattering phase function in the angle region close to π can be neglected. This region is determined by the transverse size of an instantaneous scattering volume. Using the above assumptions in the case of a point monodirectional (PM) source emitting a δ-pulse with unit energy at the time moment $t = 0$, the following expression can be obtained for the lidar return power arrived at the moment of time $t = 2z/c$ to the receiving system:

$$P(z, R_r, \gamma_r, d) = \frac{c}{4\pi} \beta_\pi(z) \int_0^\infty \nu J_0(\nu d)\, \tilde{D}(\nu, z\nu)\, F(\nu)\, d\nu, \quad (1)$$

where

$$F(\nu) = \exp\,[-2\,\tau(z) + g(\nu)]\,, \quad \tau(z) = \int_0^z \varepsilon(s)\, ds\,; \quad (2)$$

$$g(\nu) = 2\int_0^z \sigma(z - s)\, \tilde{x}(\nu s)\, ds\,; \quad (3)$$

J_0 is the first-kind Bessel function; $\tilde{D}(\nu, p)$ is the Hankel transform of the function $D(r, \gamma)$ over the variables r and γ; $F(\nu)$ is the optical transfer function (OTF) for a stationary source in a virtual medium where light scattering and extinction coefficients are twice as large as their real values $\varepsilon(s)$ and $\sigma(s)$, and the small-angle scattering phase function $\chi(\gamma)$ does not vary.

Along with the backscattering coefficient $\beta_\pi(z)$ the optical transfer function $F(\nu)$ in Eq. (1) also bears information on the optical properties of a medium and also depends on the Hankel transform of the small-angle scattering phase function $\tilde{x}(p)$. The small-angle scattering phase function $x(\gamma)$ satisfies the condition of normalization $2\pi \int_0^\infty x(\gamma)\, \gamma\, d\gamma = 1$. It is similar to the real scattering phase function in the range of small scattering angles γ and tends to zero at large γ angles. When replacing the scattering phase function by its small-angle counterpart, the value of the scattering coefficient $\sigma(s)$ is substituted by an "efficient" value. This makes it possible to consider approximately the loss of radiation scattered at large angles.

The form of the function $\tilde{D}(\nu, p)$ is determined by the spatial and angular characteristics of the receiving system. Subsequent analysis will be made for the case when the function $D(r, \gamma)$ is of a step-wise form in both variables, i.e., we assume that

$$D(r, \gamma) = U(R_r - r)\; U(\gamma_r - \gamma)\,, \quad (4)$$

where $U(r)$ is the unit step function (the Heaviside unit function), R_r and γ_r are the radius of entrance pupil and the half-angle of the receiver's field of view. The Hankel transform of the function $D(r, \gamma)$ (4) yields the following expression

$$\tilde{D}(\nu, p) = \tilde{U}(\nu, R_r)\; \tilde{U}(p, \gamma_r)\,, \quad (5)$$

where

$$\tilde{U}(\nu, R_r) = S_r \frac{2\, J_1\,(R_r\, \nu)}{R_r\, \nu}\,,$$

$$\tilde{U}(p, \gamma_r) = \Omega_r \frac{2\, J_1\,(\gamma_r\, p)}{\gamma_r\, p}\,; \quad (6)$$

$J_1(.)$ is the Bessel function of the first kind; $S_r = \pi R_r^2$ is the receiving aperture area; $\Omega_r = \pi\, \gamma_r^2$ is the solid receiving angle.

Taking into account Eqs. (4)–(6), it can be readily seen that Eq. (1) can also be presented in the form[12]:

$$P(z, R_r, \gamma_r, d) = \frac{c}{2} \beta_\pi(z)\; S_r\; \Omega_r\; E(z, R_r, \gamma_r, d)\,, \quad (7)$$

where the function $E(z, R_r, \gamma_r, d)$ describes the irradiance distribution in a virtual medium formed at a distance $z = ct/2$ when irradiated with a stationary directional source of a unit power with the exit aperture of the radius R_r and the angular beam divergence γ_r.

Equation (1) determines the lidar return power P depending on the above mentioned optical properties of the scattering medium: $\varepsilon(s)$, $\sigma(s)$, $\beta_\pi(z)$, $x(\gamma)$ and the parameters of the lidar receiving system: d, R_r, and γ_r. This equation generalizes the lidar equation with the account of multiple scattering in the small-angle approximation of the radiative transfer theory. The known approximations of low multiplicities of scattering: single and double scattering ones follow from Eq. (1). Based on formula (1), we can estimate the noise due to multiple scattering in lidar returns when interpreting sounding data in the framework of the single-scattering approximation. Since lidar returns in the small-angle approximation bear information about the optical transfer function of a medium $F(\nu)$ (2), the possibility exists of determining the OTF (and

RFF) of the medium with the use of laser sounding methods.[13] In its turn, for solving inverse problems of laser sounding on reconstruction of optical characteristics of dense media, the methods based on the interpretation of the relation $F(\nu)$ (Ref. 14 and 15) retrieved from lidar experiments can be used.

Since the behavior of OTF $F(\nu)$ is largely determined by the scattering phase function $x(\gamma)$, for solving the corresponding inverse problems the use of *a priori* model representations of its structure is of a considerable importance. Now we briefly consider the choice of a model for the small-angle scattering phase function in Eq. (1).

2. Model of the small-angle scattering phase function

At light scattering by large particles, for which $kr|m-1| \gg 1$, where r and m denote the size and the refractive index of the particle; $k = 2\pi/\lambda$, λ is the light wavelength, a satisfactory description of the scattering phase function in the range of small angles gives the Fraunhofer diffraction approximation on a plane opaque screen that coincides with the particle contour. In the case of spherical particles, this approximation results in the known Airy formula[16] for the scattering phase function $x(\gamma) = x^{(d)}(\gamma)$. At the same time, for the extinction coefficient ε and the scattering coefficient $\sigma = \sigma^{(d)}$ the relationships are fulfilled: $\varepsilon = 2S$, $\sigma^{(d)} = S$, where $S = \int_0^R s(r)\,dr$ is the total geometric cross section of particles in a unit scattering volume; $s(r)$ is the size distribution function of particle geometric cross sections. For a polydisperse ensemble of particles describing the cloud of the Cloud C–1 model from Refs. 17, the applicability of the diffraction approximation to the scattering angles within the limits $\gamma < 8°$ (at $\lambda = 0.7$ μm) is shown in Ref. 18.

The Hankel transform of the scattering phase function $x^{(d)}(\gamma)$ determines the correlation function of particle shadows $\varphi(\rho)$ (Ref. 11). It is connected with the normalized function of the particle geometric cross section size-distribution $f(r) = s(r)/S$ by the expression

$$\varphi(\rho) = \int_{\rho/2}^{R} G(\rho/2r)\, f(r)\, dr\,, \quad \int_0^R f(r)\, dr\,, \qquad (8)$$

where R is the maximum size of scatterers. The function $G(\rho/2r)$ has an obvious geometric meaning: its value equals the ratio between the area of the intersection of two circles of radius r with the distance ρ between the centers of circles to the area of one of the circles.

The allowance for light reflected by particles and transmitted through particles results in a detailed description of the scattering phase function for large particles. This question is discussed in detail in Refs. 19 and 20, where the expressions are obtained in the framework of geometric optics for the phase function of light reflected $x^{(r)}(\gamma)$ and transmitted $x^{(t)}(\gamma)$ through a particle taking into account reflection inside a particle. This enables the following expansion for the total scattering phase function

$$x(\gamma) = \frac{\sigma^{(d)}}{\sigma}\, x^{(d)}(\gamma) + \frac{\sigma^{(r)}}{\sigma}\, x^{(r)}(\gamma) + \frac{\sigma^{(t)}}{\sigma}\, x^{(t)}(\gamma) \quad (9)$$

and the scattering coefficient

$$\sigma = \sigma^{(d)} + \sigma^{(r)} + \sigma^{(t)}\,. \qquad (10)$$

For the functions $x^{(r)}(\gamma)$ and $x^{(t)}(\gamma)$ the simple approximation formulas may be found in the literature:

$$x^{(r)}(\gamma) = x^{(r)}(0)\, e^{-\alpha\gamma}\,, \quad x^{(t)}(\gamma) = x^{(t)}(0)\, e^{-\beta\gamma^2}\,, \qquad (11)$$

in which the parameters α and β depend on the refractive index of the particulate matter. As shown in literature,[21] the use of the approximation of the form (9) for $x(\gamma)$ with the allowance made for the approximations (11) enables one to describe the phase function for the cloud C1 model (Ref. 17) with the error no less than 15% within the scattering angle range $\gamma < 350$ (at $\lambda = 0.7$ μm).

The values of the components of scattering coefficient $\sigma^{(r)}$ and $\sigma^{(t)}$ due to light reflected and refracted by particles are determined by the parameters of approximation models (11) and are proportional to the geometrical cross section of particles S. This makes it possible to express the scattering coefficient $\sigma = \Lambda\varepsilon$ in terms of the extinction coefficient ε and the "effectiveB albedo of single scattering Λ, which, in turn, is also the function of the parameters α and β and may vary from 0.5 (the model of opaque screens) to 0.94 ($m = 1.33 - i\cdot 0$).

In the case of nonabsorbing particles, the phase function in the approximation of geometric optics does not depend on the medium disperse composition, and the data on the medium microstructure are contained in solely the diffraction component of the scattering phase function $x^{(d)}(\gamma)$. The absorption, if present, results in the energy loss of light in passing through a particle. The magnitude of loss depends on the trajectory of a light beam inside a particle and, finally, on its size. This gives rise to the change of the form of the phase function component $x^{(t)}(\gamma)$ and, in particular, to a decrease of its asymmetry factor.

3. Analysis of the lidar equation structure

To analyze Eq. (1), we can conveniently subdivide the OTF $F(\nu)$ written by Eq. (2) into the incident attenuated component $F_0 = e^{-2\tau(z)}$ and the scattered component $F_{sc}(\nu) = F(\nu) - F_0$. In this case and with the allowance made for Eq. (7), Eq. (1) can be modified as follows

$$P(z, R_r, \gamma_r, d) = \frac{c}{2}\, \beta_\pi(z)\, S_r\, \Omega_r\, [E_0(z, d) + E_{sc}(z, d)]\,. \qquad (12)$$

If in Eq. (12) the component $E_{sc}(z, d)$ is neglected, we obtain the lidar equation of a conventional type in the single scattering approximation

$$P_1(z, R_r, \gamma_r, d) = \frac{c}{2}\beta_\pi(z)\, S_r\, \Omega_r\, E_0(z, d)\ , \quad (13)$$

where

$$E_0(z, d) = A e^{-2\tau(z)} \int_0^\infty \nu^{-1} J_0(\nu d)\, J_1(\nu R_r)\, J_1(\nu z \gamma_r)\, d\nu\ , \quad (14)$$

$$A = 2/(\pi\, R_r\, z\, \gamma_r)\ .$$

The integral term in Eq. (14) describes the influence of the geometric factor entering into the lidar equation in the single scattering approximation.

Formula (12) can be also presented in the form

$$P(z) = P_1(z)\,[1 + m(z)]\ , \quad (15)$$

where the function $m(z)$ is the ratio between the multiply and singly scattered components of a lidar return

$$m(z) = \frac{P(z) - P_1(z)}{P_1(z)} = \frac{E_{sc}(z, d)}{E_0(z, d)}\ . \quad (16)$$

Before analyzing the general equation (1), we consider briefly the structure of the lidar return in the single scattering approximation (13).

3.1. Single scattering approximation

In this approximation the lidar return $P_1(z)$ (13) is determined by only two optical characteristics of a scattering medium: the extinction coefficient $\varepsilon(z)$ and the backscattering coefficient $\beta_\pi(z)$. It is worth noting here some peculiarities of the effect of the geometric factor in Eq. (13), following from the characteristics of the integral of the Bessel functions product in Eq. (14). This integral, as shown in Refs. 22 and 23, is expressed in terms of elementary functions. According to Ref. 23, the lidar return $P_1(z)$ (13) can be presented as

$$P_1(z) = (c/2)\,\beta_\pi(z)\, e^{-2\tau(z)}\, z^{-2}\, G(R_r, z\gamma_r, d)\ , \quad (17)$$

where the function $G(R_r, z\gamma_r, d)$ is a two-dimensional contraction of circles with the radii R_r and $z\gamma_r$. The distance between the centers of circles equals d.

Depending on the relationship between the parameters d, R_r, and γ_r, the sounding path can be divided into the characteristic regions or zones, namely, the near, intermediate, and far zone; within the limits of these zones the calculations connected with the account of geometry of a lidar experiment may be simplified.

In the far zone being of principal practical interest at

$$z\gamma_r > R_r + d, \quad (18)$$

the geometrical factor is constant and equal to the area of the receiving aperture $G = S_r$, hence the power of a received signal is determined by the formula

$$P_1(z) = (c/2)\, z^{-2}\, \Omega_r\, \beta_\pi(z)\, e^{-2\tau(z)}\ . \quad (19)$$

This equation is well understood, and there are many publications on the methods of its inversion (see, for example, the review in Ref. 1).

In the near zone determined from the condition

$$z\gamma_r < |\, R_r - d\,|, \quad (20)$$

at $d > R_r$ we obtain $G = 0$ and, hence, $P_1(z) = 0$. At $d < R_r$ the geometrical factor in the near zone increases according to the square law $G = \pi(z\gamma_r)^2$. This results in the exclusion of the factor z^{-2} in the equation for the lidar return power:

$$P_1(z) = (c/2)\,\Omega_r\,\beta_\pi(z)\, e^{-2\tau(z)}\ . \quad (21)$$

In the intermediate zone

$$|\, R_r - d\,| < z\gamma_r < R_r + d, \quad (22)$$

the geometrical factor G is a monotonically increasing function z, which varies from $\pi(R_r - d)^2$ to πR_r^2. In the integrated scheme of sounding at $d = 0$ the intermediate zone length reduces to zero.

3.2. Correction for multiple scattering

With the allowance made for the form of the function $E_0(z, d)$ (14) in the far zone (18), the ratio between the multiply and singly scattered components of a lidar return $m(z)$ (16) can be written in the following form[12]:

$$m(z) = \frac{2z\gamma_r}{R_r} \int_0^\infty \nu^{-1} J_0(\nu d) J_1(\nu R_r) J_1(\nu z\gamma_r)\,[e^{g(\nu)} - 1]\, d\nu. \quad (23)$$

In particular, for a monostatic coaxial scheme of the lidar transmitter and receiver ($d = 0$) it follows from Eq. (23), at $R_r \to 0$, that

$$m(z) = z\gamma_r \int_0^\infty J_1(\nu z\gamma_r)\,[e^{g(\nu)} - 1]\, d\nu\ . \quad (24)$$

The expression in the right-hand side of Eq. (24) is absolutely identical to the formula determining the relationship of fluxes of scattered and direct radiation penetrating through a circular area of the radius ($z\gamma_r$) in the case of a TM-source.[12]

In the near zone (20) the formula for $m(z)$ takes the form analogous to Eq. (23), if the parameters R_r and ($z\gamma_r$) in the factor before the integral change their places. At $d = 0$ and $\gamma_r \to 0$ in the near zone we have

$$m(z) = z\gamma_r \int_0^\infty J_1(\nu R_r)\,[e^{g(\nu)} - 1]\, d\nu\ . \quad (25)$$

4. Results of numerical simulation

As an example, Fig. 1 shows a typical parametric series of characteristics $m(\gamma_r)$ calculated at different optical thickness τ of a homogeneous 1-km layer; the distance H to the near boundary of the layer is 1 km. For the above-listed data the scattering phase function is chosen in the Fraunhofer diffraction approximation $x(\gamma) = x^{(d)}(\gamma)$ ($\Lambda = 0.5$) at $\lambda = 0.55$ μm for a polydisperse ensemble of particles of the C1 Cloud type with the effective particle size R_{eff}. A modal radius of 10 μm is considered as R_{eff}.

The characteristic $m(\gamma_r)$ increases monotonically as a function of the angle γ_r and tends to the limit $m_\infty = \exp(2\Lambda\tau) - 1$ at $\gamma_r \to \infty$, whence it follows that even at the optical thickness $\tau = 1$ the contribution of multiply scattered radiation to the lidar return may dominate at a sufficiently large angle of the receiver's field of view γ_r. With the increasing τ the ratio between the multiply and singly scattered components of a lidar return may reach the value of several tens. Under such conditions the value of single scattering signal may occur at the level of (and less than) the measurement errors in a total lidar return. This produces a negative effect on the accuracy of experimental data interpretation based on single scattering analysis of lidar signals and imposes a limitation on the choice of admissible values of the angle γ_r. For the characteristics depicted in Fig. 1, the threshold value of the angle γ_r, within which the function $m(\gamma_r) \le m_1$, is presented in Fig. 2 as a function of optical thickness τ at $m_1 = 10$ (curve *1*). This curve has the vertical asymptote $\tau = \ln 11 \cong 2.4$. The similar dependence of $\gamma_r(\tau)$ for $m_1 = 5$ and 2 is presented in Fig. 2 by curves *2* and *3*, respectively.

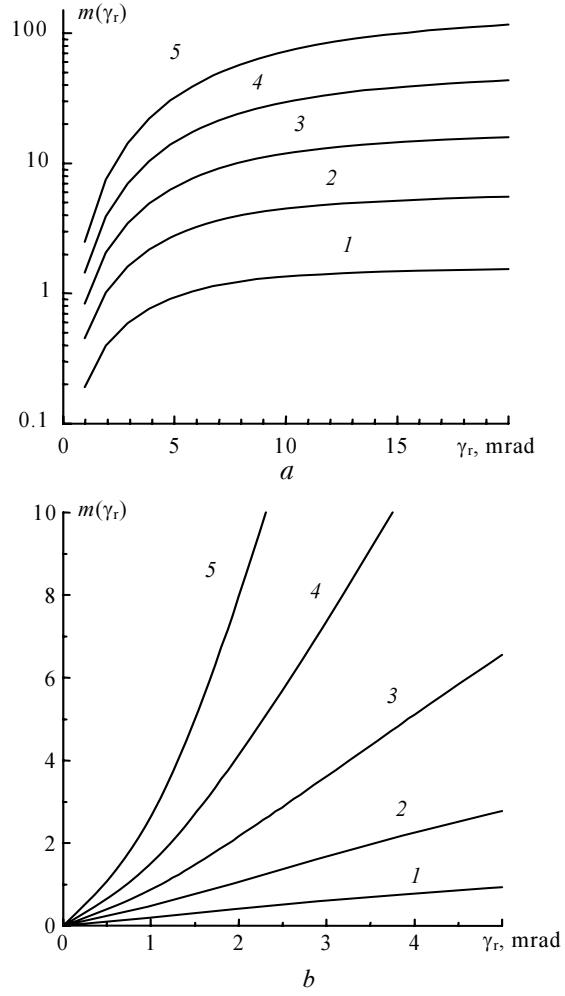

Fig. 1. Variability of the function $m(\gamma_r)$ at a depth of 1 km inside a 1-km far homogeneous layer at variations of the optical thickness $\tau = 1, 2, \ldots, 5$ (curves *1–5*).

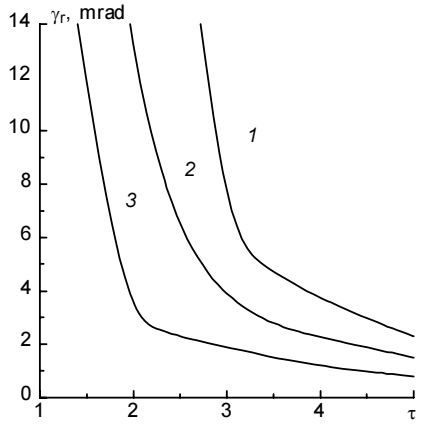

Fig. 2. Isoline chart of the function $m(\tau, \gamma_r) = 10(1), 5(2), 2(3)$ based on the data from Fig. 1.

The dependences given in Figs. 1 and 2 are obtained for the small-angle scattering phase function $x(\gamma) = x^{(d)}(\gamma)$ in the diffraction approximation, which describes satisfactorily the lidar return structure at relatively small angular apertures. The geometric-optics component in the scattering phase function plays important part at the periphery of a beam, what is illustrated in Figs. 3 and 4. Figure 3 shows as an example the dependence of $m(\gamma_r)$ at two values $\tau = 2$ and 3 calculated without (curves *1*, *2*) and with (curves *1′*, *2′*) the account of the above component ($m(\gamma_r) = m^{(d)}(\gamma_r)$) enabling one to assess the angular range γ_r, within which the small-angle scattering phase function in the diffraction approximation applies to lidar returns. Figure 4 shows the dependence on the optical thickness τ for the angles γ_r, where the discrepancy between the functions $m^{(d)}(\gamma_r)$ and $m(\gamma_r)$ does not exceed 5, 10, and 15% (curves *1–3*, respectively).

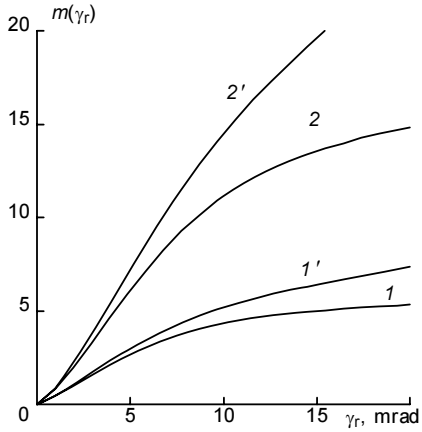

Fig. 3. A comparison between the behavior of the function $m(\gamma_r)$ calculated without (curves *1*, *2*) and with (curves *1′*, *2′*) the account of geometric optics component of the scattering phase function for two values of the optical thickness $\tau = 2$ (*1*, *1′*), 3 (*2*, *2′*) at the layer position similar to the data in Fig. 1.

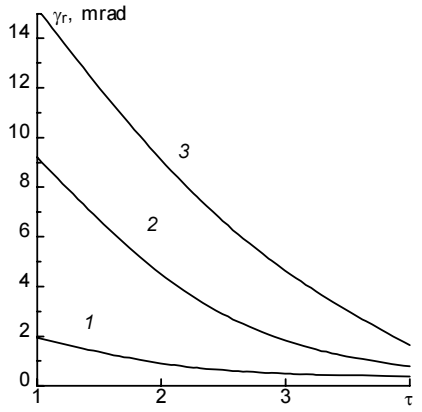

Fig. 4. The range of values of optical thicknesses τ and the receiver field-of-view angles γ_r, within which the difference between the functions $m(\gamma_r)$ and $m^{(d)}(\gamma_r)$ does not exceed 5, 10, and 15% (curves *1–3*, respectively).

The influence of the layer inhomogeneity on the behavior of function $m(\gamma_r)$ is shown in Figs. 5 and 6. Figure 5 gives the dependence of $m(\gamma_r)$ for the model of a linearly increasing extinction coefficient profile

$$\varepsilon(z) = h(z - z_0)\ ,\ z > z_0\ ,\ z = 3\ \text{km},\ z_0 = 1\ \text{km}, \qquad (26)$$

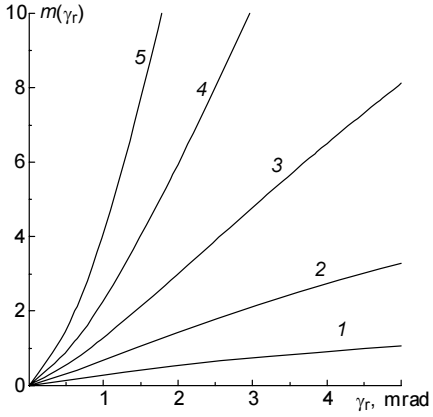

Fig. 5. Variability of the function $m(\gamma_r)$ at a depth of 2 km at variations of the rate of linear increase of the extinction coefficient inside the layer; curves *1–5* correspond to the optical thickness τ = 1, 2,..., 5.

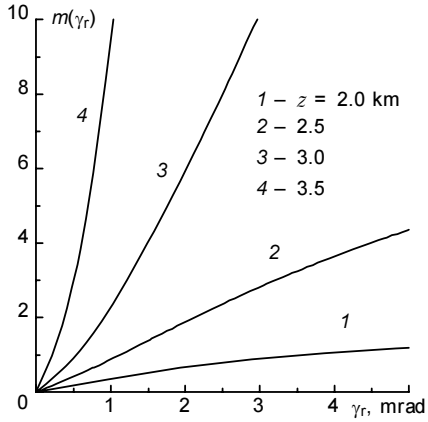

Fig. 6. Transformation of the function $m(\gamma_r)$ as the beam penetrates deep into the layer with linearly increasing profile of the extinction coefficient; the value τ = 1 corresponds to curve *1* (*z* = 2 km).

in the case when the layer limits are fixed and the rate of increase of the extinction coefficient determined by the coefficient *h* varies.

Figure 6 shows the transformation of the angular structure of the function $m(\gamma_r)$ for linear model of the profile of the extinction coefficient $\varepsilon(z)$ (26) at $h = 2$ as the beam penetrates into the layer. As seen from comparison of Figs. 5 and 6 with Fig. 1, the behavior of the functions $m(\gamma_r)$ undergoes slight qualitative changes at variations of the model of the extinction coefficient profile $\varepsilon(z)$. The results referring to analysis of applicability limits of the diffraction approximation of the scattering phase function and selection of the receiver's field-of-view angle γ_r to provide for a permissible level of multiple scattering background also appear very close in behavior.

The further generalization of numerical results is possible based on the properties of similarity that may be obtained for Eq. (1). Taking into account the constant characteristics of $m(\gamma_r)$ for a fixed value of the dimensionless parameter

$$p = \frac{R_e\, z}{\lambda\, H}\,\gamma_r\ , \qquad (27)$$

all the above-mentioned data are simply generalized for a wide range of models corresponding to the different distance *z*, the geometric thickness of the layer *H* and having similar distribution functions $f(\eta)$ in relative size of particles $\eta = r/R_e$. Thus, for example, if the scattering layer is located at a distance *z′*, all other parameters being invariable, the function $m(\gamma_r)$ is transformed according to the rule

$$m(z',\ \gamma_r) = m\ (z,\ \gamma_r z'/z)\ , \qquad (28)$$

i.e. displacement of the layer does not change the angular structure of the lidar return accurate to the scale transformation over the variable γ_r, being inversely related to the variation of the distance *z*. It follows herefrom that as the distance from a lidar to the scattering layer increases, the multiple scattering background from the same depth of the layer grows following the law determined by Eq. (28).

5. Conclusion

Thus, this paper considers the equation describing the behavior of the lidar return power depending on the microstructure of a coarse disperse medium and geometric parameters of the experimental scheme with the account of multiple scattering in the small-angle approximation. The radius of the receiving aperture, the angle of the receiver field of view, as well as the distance between the optical axes of the source and the receiver are considered as geometric parameters. The influence of the disperse composition of the medium manifests itself as the correlation function of a particle shadow, which represents the Hankel transform from a diffraction component of the small-angle phase function.

The paper presents some results of calculations of the relationship between the components of multiply

and singly scattered radiation in the lidar return for the models of a homogeneous layer and a layer with a linearly increasing profile of the extinction coefficient.

The permissible angles of the receiver's field of view are estimated. Within these angles the contribution of multiply scattered radiation exceeds the contribution of singly scattered radiation by the factor no more than 2, 5, and 10 for layers of variable optical thickness. For the case of lidar returns calculated with the account of multiple scattering, the applicability of the diffraction approximation to description of the small-angle part of the scattering phase function has been studied numerically.

Using the similarity relationships, the results of numerical calculations are extended to a wide range of models with various modal radii of particles, different distance to the near layer boundary, and different penetration depth into a layer.

References

1. V.E. Zuev, G.M. Krekov, and M.M. Krekova, in: *Remote Sensing of the Atmosphere* (Novosibirsk, Nauka, 1978), pp. 3–46.
2. J.D. Klett, Appl. Opt. **20**, 211–220 (1981).
3. J.A. Ferguson and D.H. Stephens, Appl. Opt. **22**, 3673–3675 (1983).
4. V.A. Korshunov, Atm. Opt. **3**, No. 2, 101–107 (1990).
5. Q. Jinhuan, H. Quenzel, and M. Wiegner, in: *Abstracts of Papers at 15 International Laser Radar Conference*, Tomsk, USSR (1990), Part 1, pp. 345–348.
6. L.S. Dolin, Izv. Vyssh. Uchebn. Zaved., Radiofizika **7**, No. 2, 380–382 (1964).
7. D.M. Bravo-Zhivotovskii, L.S. Dolin, A.G. Luchinin, and V.A. Savel'ev, Izv. Akad. Nauk SSSR, Fiz. Atmos. Okeana **5**, No. 2, 160–170 (1969).
8. B.V. Ermakov and Yu.A. Il'inskii, Izv. Vyssh. Uchebn. Zaved., Radiofizika **12**, No. 5, 694–701 (1969).
9. L.S. Dolin and V.A. Savel'ev, Izv. Akad. Nauk SSSR, Fiz. Atmos. Okeana **7**, No. 5, 505–510 (1971).
10. A.N. Kozhevnikov and V.M. Orlov, in: *Abstracts of Reports at the First All-Union Conference on Atmospheric Optics*, Tomsk (1976), Part 1, pp. 368–372.
11. V.F. Belov, A.G. Borovoy, N.I. Vagin, and S.N. Volkov, Izv. Akad. Nauk SSSR, Fiz. Atmos. Okeana **20**, No. 3, 323–327 (1984).
12. V.E. Zuev, V.V. Belov, and V.V. Veretennikov, *Theory of Systems in Optics of Dispersed Media* (Spektr, Tomsk, 1997), 402 pp.
13. V.V. Veretennikov, in: *Abstracts of Reports at the Second All-Union Symposium on Atmospheric and Oceanic Optics*, Tomsk (1995), Part 2, pp. 320–321.
14. V.V. Veretennikov, Atmos. Oceanic Opt. **6**, No. 9, 601–604 (1993).
15. V.V. Veretennikov, Atmos. Oceanic Opt. **6**, No. 4, 250–254 (1993).
16. M. Born and E. Wolf, *Principles of Optics* (Pergamon Press, Oxford–London–Edinburgh–NewYork–Paris–Frankfurt, 1964).
17. D. Deirmendjian, *Scattering of Electromagnetic Radiation on Spherical Polydispersions* (Elsevier, New York, 1969).
18. A.S. Drofa and A.S. Usachev, Izv. Akad. Nauk SSSR, Fiz. Atmos. Okeana **16**, No. 9, 933–938 (1980).
19. K.S. Shifrin, *Light Scattering in Turbid Medium* (Gostekhteorizdat, Moscow, 1951), 288 pp.
20. C. Bohren and D. Huffman, *Absorption and Scattering of Light by Small Particles* (Willey, New York–Chichester–Brisbane–Toronto–Singapore, 1983).
21. E.P. Zege and A.A. Kokhanovskii, Izv. Akad. Nauk SSSR, Fiz. Atmos. Okeana **30**, No. 6, 812–818 (1994).
22. V.V. Veretennikov, in: *Abstracts of Reports at the Fourth Symposium on Atmospheric and Oceanic Optics*, Tomsk (1997), pp. 173–174.
23. V.V. Veretennikov, Atmos. Oceanic Opt. **11**, No. 9, 858–862 (1998).